

1 Predicted Coronavirus Nsp5 Protease Cleavage Sites in the 2 Human Proteome: A Resource for SARS-CoV-2 Research

3 Benjamin M. Scott^{1,2*}, Vincent Lacasse³, Ditte G. Blom⁴, Peter D. Tonner⁵, Nikolaj S. Blom⁶

4 1 Associate, Biosystems and Biomaterials Division, National Institute of Standards and Technology,
5 Gaithersburg, Maryland, USA.

6 2 Department of Chemistry and Biochemistry, University of Maryland, College Park, Maryland, USA.

7 3 Segal Cancer Proteomics Centre, Lady Davis Institute, Jewish General Hospital, McGill University, Montreal,
8 Quebec, Canada

9 4 Department of Applied Mathematics and Computer Science, Technical University of Denmark, Lyngby,
10 Denmark.

11 5 Statistical Engineering Division, National Institute of Standards and Technology, Gaithersburg, Maryland, USA

12 6 Department of Bioengineering, Kongens Lyngby, Technical University of Denmark

13 *Corresponding author, ben_scott@outlook.com

14 BMS current affiliation: Concordia University, Centre for Applied Synthetic Biology, Montreal, Quebec, Canada

15

16

17 18 19 Abstract

20 **Background:** The coronavirus nonstructural protein 5 (Nsp5) is a cysteine protease required for
21 processing the viral polyprotein and is therefore crucial for viral replication. Nsp5 from several
22 coronaviruses have also been found to cleave host proteins, disrupting molecular pathways
23 involved in innate immunity. Nsp5 from the recently emerged SARS-CoV-2 virus interacts with
24 and can cleave human proteins, which may be relevant to the pathogenesis of COVID-19.

25 Based on the continuing global pandemic, and emerging understanding of coronavirus Nsp5-
26 human protein interactions, we set out to predict what human proteins are cleaved by the
27 coronavirus Nsp5 protease using a bioinformatics approach.

28 **Results:** Using a previously developed neural network trained on coronavirus Nsp5 cleavage
29 sites (NetCorona), we made predictions of Nsp5 cleavage sites in all human proteins. Structures
30 of human proteins in the Protein Data Bank containing a predicted Nsp5 cleavage site were
31 then examined, generating a list of 92 human proteins with a highly predicted and accessible
32 cleavage site. Of those, 48 are expected to be found in the same cellular compartment as Nsp5.
33 Analysis of this targeted list of proteins revealed molecular pathways susceptible to Nsp5
34 cleavage and therefore relevant to coronavirus infection, including pathways involved in mRNA
35 processing, cytokine response, cytoskeleton organization, and apoptosis.

36 **Conclusions:** This study combines predictions of Nsp5 cleavage sites in human proteins with
37 protein structure information and protein network analysis. We predicted cleavage sites in
38 proteins recently shown to be cleaved *in vitro* by SARS-CoV-2 Nsp5, and we discuss how other
39 potentially cleaved proteins may be relevant to coronavirus mediated immune dysregulation.
40 The data presented here will assist in the design of more targeted experiments, to determine the
41 role of coronavirus Nsp5 cleavage of host proteins, which is relevant to understanding the
42 molecular pathology of SARS-CoV-2 infection.

43 **Keywords:** Nsp5, Mpro, 3CL, protease, coronavirus, human proteins, human proteome, SARS-
44 CoV-2, COVID-19.

45

46

47 **Background**

48 Coronaviruses are major human and livestock pathogens, and are the current focus of
49 international attention due to an ongoing global pandemic caused by severe acute respiratory
50 syndrome coronavirus 2 (SARS-CoV-2). This recently emerged coronavirus likely originated in
51 bats in China, before passing to humans in late 2019 through a secondary animal vector [1, 2].
52 Although 79% identical at the nucleotide level to SARS-CoV [2], differences in the infectious
53 period and community spread of SARS-CoV-2 has caused a greater number of cases and
54 deaths worldwide [3, 4]. Individuals infected by SARS-CoV-2 can develop COVID-19 disease
55 which primarily affects the lungs, but can also cause kidney damage, coagulopathy, liver
56 damage, and neuropathy [5-10]. Hyperinflammation, resulting from dysregulation of the immune
57 response to SARS-CoV-2 infection, has emerged as a leading hypothesis regarding severe
58 COVID-19 cases, which may also explain the diverse and systemic symptoms observed [11-14].

59 Similar to other coronaviruses, once a cell is infected, the 5' portion of the SARS-CoV-2
60 (+)ssRNA genome is translated into nonstructural proteins (Nsps) required for viral replication,
61 which are expressed covalently linked to one another (Fig. 1a) [15]. This polyprotein must
62 therefore be cleaved to free the individual Nsps, which is performed by two virally encoded
63 proteases: Nsp3/papain-like protease (PLpro) and Nsp5/Main Protease (Mpro)/3C-like protease
64 (3CLpro). Nsp5 is responsible for the majority of polyprotein cleavages and its function is
65 conserved across coronaviruses [16, 17], making it a key drug target as its inhibition impedes
66 viral replication (reviewed by [18]).

67 All coronavirus Nsp5 proteases identified to date are cysteine proteases in the
68 chymotrypsin family, which primarily cleave peptides at P2-P1-P1' residues leucine-glutamine-

69 alanine/serine [16, 17, 19, 20], where the cleavage occurs between the P1 and P1' residues.
70 Nsp5 forms a homodimer for optimal catalytic function but may function as a monomer when
71 processing its own excision from the polyprotein [21-23]. SARS-CoV-2 Nsp5 shares 96.1%
72 sequence identity with SARS-CoV Nsp5 and has similar substrate specificity *in vitro*, but SARS-
73 CoV-2 Nsp5 accommodates more diverse residues at substrate position P2 and may have a
74 higher catalytic efficiency [22-25].

75 Coronavirus proteases also manipulate the cellular environment of infected cells to favor
76 viral replication [26, 27], and disrupt host interferon (IFN) signaling pathways to suppress the
77 anti-viral response of the innate immune system (reviewed by [28-30]). The role of coronavirus
78 protease Nsp3 as an IFN antagonist has been well documented, including SARS-CoV-2 Nsp3
79 [31, 32]. Although Nsp3 proteolytic activity contributes to IFN antagonism, it is the
80 deubiquitinating and deISGylating activities of Nsp3 that are primarily responsible [32-39]. In
81 contrast, fewer examples of Nsp5 mediated disruption of host molecular pathways have been
82 identified, and all are a result of its proteolytic activity [40-43].

83 SARS-CoV-2 Nsp5 antagonism of IFN is not yet clear [31, 44, 45], but *in vitro* evidence
84 supports SARS-CoV-2 Nsp5 mediated cleavage of TAB1 and NLRP12 which are involved in
85 innate immunity [46]. Hundreds of potentially cleaved peptides containing the Nsp5 consensus
86 sequence appeared when lysate from human cells were incubated with recombinant Nsp5 from
87 SARS-CoV, SARS-CoV-2, or hCoV-NL63, indicating a significant potential for Nsp5 mediated
88 disruption of host proteins [47]. Similarly, the abundance of potentially cleaved peptides
89 containing a Nsp5 consensus sequence was increased in cells infected *in vitro* with SARS-CoV-
90 2, which was dependent on the cell type studied [48]. Knock down or inhibition of some of these
91 human proteins likely cleaved by Nsp5, suppressed SARS-CoV-2 replication *in vitro*, suggesting
92 that targeted host protein proteolysis is involved in viral replication [48]. Many other SARS-CoV-
93 2 Nsp5-host protein interactions have been identified using proximity labeling and co-
94 immunoprecipitation [49-54], but it is unknown if these interactions lead to Nsp5 mediated
95 cleavage. Indeed, *in vitro* studies may miss Nsp5-host protein interactions due to cleavage of
96 the host protein upon Nsp5 binding [49], and because individual cell types only express a limited
97 set of human proteins. A proteome-wide prediction of coronavirus Nsp5 mediated cleavage of
98 human proteins is therefore relevant to understanding COVID-19 pathogenesis, and how
99 coronaviruses in general disrupt host biology.

100 The neural network NetCorona was previously developed in 2004, and was trained on a
101 dataset of Nsp5 cleavage sites from seven coronaviruses including SARS-CoV [55]. NetCorona
102 outperforms traditional consensus motif-based approaches for identifying cleavage sites, and

103 based on the similar specificities of SARS-CoV and SARS-CoV-2 Nsp5, we believed it could be
104 applied to the study of SARS-CoV-2 Nsp5 interactions with human proteins. However,
105 NetCorona only analyzes the primary amino acid sequence to predict cleavage sites, which
106 lacks information about the 3D structure of the folded protein, and therefore how exposed a
107 predicted cleavage site is to a protease. In particular, the solvent accessibility of a peptide motif
108 is closely related to proteolytic susceptibility [56, 57], and *in silico* measurement of solvent
109 accessibility has previously been used to help predict proteolysis [58-60].

110 In this study we used NetCorona to make predictions of Nsp5 cleavage sites across the
111 entire human proteome, and additionally analyzed available protein structures *in silico* to identify
112 highly predicted cleavage sites. We extended this analysis to examine subcellular and tissue
113 expression patterns of the proteins predicted to be cleaved, and applied protein network
114 analysis to identify potential key pathways disrupted by Nsp5 cleavage. Predicted Nsp5
115 cleavage sites in human proteins were similar to those recently identified *in vitro*, and human
116 proteins predicted to be cleaved by Nsp5 were found to be involved in molecular pathways that
117 may be relevant to the pathogenesis of COVID-19 disease.

118

119

120 **Results**

121 **Evaluating NetCorona Performance with the SARS-CoV-2 Polyprotein**

122 As the NetCorona neural network was not trained on the SARS-CoV-2 polyprotein sequence
123 (Fig. 1a), we first examined if the 11 polyprotein cleavage sites homologous to SARS-CoV
124 would be correctly scored as cleaved (NetCorona score >0.5). Due to the high sequence
125 similarity with SARS-CoV, there were only three cleavage sites containing different residues
126 (Fig. 1b). The mean NetCorona score for 10 out of the 11 SARS-CoV-2 Nsp5 cleavage sites
127 was 0.859 (SD = 0.08), indicating highly predicted cleavages. The cleavage site at Nsp5-Nsp6
128 was classified as uncleaved, with a score of 0.458. SARS-CoV contains the same unique
129 phenylalanine at position P2 of Nsp5-Nsp6, but with different P1'-P3' residues, and received a
130 marginal score of 0.607 in the original NetCorona paper [55]. Phenylalanine at P2 is not found in
131 other coronaviruses that infect humans [20, 61], nor in the other viruses used to train
132 NetCorona, which contributed to these low scores. A P2 phenylalanine may be intentionally
133 unfavorable at the Nsp5-Nsp6 cleavage site, to assist in its autoprocessing from the
134 polypeptide, by limiting the ability of the cleaved peptide's C-terminus to bind the Nsp5 active
135 site [61]. Interestingly, the swapped identity of the P3 and P2 residues at the SARS-CoV-2

136 Nsp10-Nsp11 cleavage site resulted in a higher score versus SARS-CoV (0.865 vs 0.65), due to
137 leucine being more common at P2 versus methionine. This mutation may result in a more rapid
138 cleavage at this site in SARS-CoV-2 versus SARS-CoV, as Nsp5 favors leucine above all other
139 residues at P2 [17, 25].

140 To investigate if NetCorona can distinguish between cleaved and uncleaved motifs,
141 NetCorona scores for all glutamine motifs in the SARS-CoV-2 1ab polyprotein were also
142 determined. To gather context from the ongoing pandemic and to investigate glutamine motifs
143 across different viral variants, 8017 SARS-CoV-2 1ab polyprotein sequences obtained from
144 patient samples were scored with NetCorona (Fig. 1c, Additional File 1: Table S1). Apart from
145 two motifs present in only 40 sequences, all glutamine motifs not naturally processed by Nsp5
146 received a NetCorona score <0.5, indicating they were correctly predicted not to be cleaved.
147 Mutations at native Nsp5 cleavage sites were also rare, with only 28 such mutated cleavage
148 sites present in 63 sequences. Except for three mutations present in one sequence each,
149 mutations at native Nsp5 cleavage sites were conservative and only modestly changed the
150 NetCorona score. One sequence contained a histidine at Nsp8-Nsp9 P1 (QIO04366), resulting
151 in NetCorona not scoring the motif. SARS-CoV and SARS-CoV-2 Nsp5 may be able to cleave
152 motifs with histidine at P1, albeit with reduced efficiency [17, 47].

153 These combined results indicate that despite NetCorona not being trained on the SARS-
154 CoV-2 sequence, it was able to correctly distinguish between cleaved versus uncleaved motifs
155 in the 1ab polyprotein, except for Nsp5-Nsp6. The rarity of mutated canonical cleavage sites
156 and mutations introducing new cleavage sites (0.8% and 0.5% of sequences respectively),
157 indicates stabilizing selection for a distinction between Nsp5 cleavage sites and all other
158 glutamine motifs.

159

160 **NetCorona Predictions of Nsp5 Cleavage Sites in the Human Proteome**

161 To generate a global view of Nsp5 cleavage sites in the human proteome, datasets were batch
162 analyzed using NetCorona (Fig. 2). Every 9-residue motif flanking a glutamine was scored,
163 where glutamine acts as P1 and four resides were analyzed on either side (P5-P4'). Using a
164 NetCorona score cutoff of >0.5, 15057 proteins (~20%) in the “All Human Proteins” dataset
165 contained a predicted cleavage site, 6056 (~29%) proteins in the “One Protein Per Gene”, and
166 2167 (~32%) proteins in the “Proteins With PDB” dataset (Additional File 1: Table S2-S4, raw
167 data sets in Additional File 2-4).

168 To help interpret these results, we compared the output from “One Protein Per Gene” to
169 proteins that have been directly tested *in vitro* for cleavage by a coronavirus Nsp5 protease

170 (Additional File 1: Table S5). There are six human proteins where cleavage sites have been
171 mapped to the protein sequence (GOLGA3, NEMO, NLRP12, PAICS, PNN, TAB1) [40, 46, 48],
172 and also two proteins from pigs (NEMO, STAT2) [41, 43], and one from cats (NEMO) [42].
173 NetCorona accurately scored 6 out of the 12 unique cleavage sites mapped in these proteins.
174 NetCorona struggled with an identical cleavage motif at Q231 in NEMO from cats, pigs, and
175 humans, which contains an uncommon valine at P1'. Interestingly, NetCorona predicted a
176 cleavage site in PNN at Q495, which was not identified in the original study but matches the
177 size of a reported secondary cleavage product [48].

178 Instances where NetCorona predicted cleavages but they are not observed *in vitro* are
179 also relevant to interpreting the full proteome results. NetCorona predicted cleavage sites in 22
180 of the 71 proteins Moustaqil *et al.* studied, however only TAB1 and NLRP12 were observed to
181 be cleaved by SARS-CoV-2 Nsp5 [46]. NetCorona predicted three cleavage sites in TAB1 and
182 two in NLRP12, but just one predicted site in each protein matched the mapped cleavage sites.

183 Many other potential cleavage sites have been identified by Koudelka *et al.* [47], where
184 N-terminomics was used to identify possible cleavage sites, after cell lysate was incubated with
185 various coronavirus Nsp5 proteases. Out of the 383 unique peptides where a glutamine was at
186 P1, NetCorona predicted that 167 (44%) of them would be cleaved (Additional File 1: Table S6).
187 Meyer *et al.* similarly used N-terminomics to study potential Nsp5 cleavage events, following *in*
188 *vitro* infection with SARS-CoV-2 [48]. They identified 12 motifs in human proteins that were
189 likely cleaved by Nsp5, of which NetCorona predicted 8 of these to be cleaved (Additional File 1:
190 Table S7).

191 Several SARS-CoV-2 human protein interactomes have been made available [49-54],
192 where interactions between Nsp5 and human proteins have been reported. Interactions
193 identified by Samavarchi-Therani *et al.* were the most numerous, and the data was well
194 annotated [51], which enabled a comparison to our results. These interaction scores, which
195 varied depending on where the BiOID tag was located on Nsp5 (Nsp5 C-term, N-term, or N-term
196 on the C145A catalytically inactive mutant), were plotted against the NetCorona score from our
197 study, which is illustrated in Additional File 5: Figure S1 (raw data in Additional File 1: Table S8).
198 Although statistically significant, the negative correlation between the strength of the Nsp5-
199 human protein interaction and the maximum NetCorona score was small: p ranged from -0.18 to
200 -0.29, r^2 ranged from 0.03 to 0.08, depending on where the BiOID tag was located on Nsp5.
201 When examining only the human proteins with a positive interaction score, the mean NetCorona
202 score ranged from 0.35 to 0.38 (SD = 0.25). Thus, Nsp5-human protein interactions identified *in*

203 *vitro* by Samavarchi-Therani *et al.* did not reflect an increased likelihood of cleavage predicted
204 by NetCorona.

205

206 **Structural Characterization of Predicted Nsp5 Cleavage Sites**

207 We next sought to incorporate available structural information of potential protein substrates into
208 our analysis, to address the discrepancy between the cleavage events predicted by NetCorona,
209 and mapped cleavage sites that have been directly observed *in vitro*. The “Proteins With PDB”
210 dataset contains only human proteins that have a solved structure available in the RCSB
211 Protein Data Bank (PDB), however technical limitations for solving protein structures means that
212 certain protein domains, such as transmembrane and disordered regions, may be
213 underrepresented [62]. To investigate if the available PDB structures contained a biased
214 distribution of NetCorona scores, similarity between the distribution of NetCorona scores for
215 “Proteins With PDB” and proteins in the other two datasets was assessed through the non-
216 parametric KS test (Fig. 3a). There was insufficient evidence to reject the null hypothesis that
217 the distribution of scores for “Proteins With PDB” proteins was equivalent to scores for “All
218 Human Proteins” and “One Protein Per Gene” ($p=0.121$ and $p=0.856$, respectively), indicating
219 that there was not significant bias in the distribution of NetCorona scores.

220 NetCorona scores are derived from the primary amino acid sequence, but targeted
221 proteolysis is also dependent on the 3D structural context of the potential substrate peptide
222 within a protein [56, 57]. Many methods have been developed to quantify this structural context
223 *in silico*, and solvent accessibility has been shown to be a strong predictor of proteolysis [57].
224 Accessible surface area (ASA) is commonly used to measure solvent accessibility, where a
225 probe that approximates a water molecule is rolled around the surface of the protein, and the
226 path traced out is the accessible surface [63]. Thin slices are then cut through this path, to
227 calculate the accessible surface of individual atoms. After obtaining PDB files containing motifs
228 predicted to be cleaved by NetCorona, the total ASA of each 9 amino acid motif was calculated
229 using Protein Structure and Interaction Analyzer (PSAIA) [64]. This ASA was then multiplied by
230 the motif’s NetCorona score to provide a “Nsp5 access score”, which represents both the
231 solvent accessibility and substrate sequence preference. A Nsp5 access score was obtained for
232 914 glutamine motifs in 794 unique human proteins (Additional File 1: Table S9), with the
233 process for selecting PDB files to analyze listed in Additional File 6.

234 Specific examples are presented to illustrate the utility of the Nsp5 access score (Fig.
235 3b-e). Acetylcholinesterase (ACHE) contains a motif at Q259 that was highly scored by
236 NetCorona (0.890), but due to its presence in a tightly packed beta sheet in the core of the

237 protein, the low ASA (38.4 \AA^2) results in a similarly low Nsp5 access score (34.1) and is
238 therefore unlikely to be cleaved by Nsp5 (Fig. 3b). TGF-beta-activated kinase 1 (TAB1) is one of
239 the few human proteins with a structure and experimental evidence of SARS-CoV-2 cleavage at
240 specific sites (Q132 and Q444) [46]. As illustrated in Fig. 3c, the nearby motif at Q108 was
241 scored higher than Q132 by NetCorona, but the greater ASA of the Q132 motif contributes to a
242 higher Nsp5 access score, which matches the experimental evidence. The human protein with
243 the highest Nsp5 access score was DEAH box protein 15 (DHX15), as the motif surrounding
244 Q788 was both highly scored by NetCorona and its location proximal to the C-terminus of the
245 protein makes it highly solvent exposed (Fig. 3d).

246

247 **Rationale for Nsp5 Access Score Cut-Off**

248 To focus analysis on human proteins most likely to be cleaved by Nsp5, we determined a
249 relevant cut-off to the Nsp5 access score. Using available structures and homology models, the
250 Nsp5 access score of SARS-CoV-2 native cleavage sites was calculated, which ranged from
251 487 (Nsp15-Nsp16) to 923 (Nsp4-Nsp5) (Additional File 1: Table S10). The Nsp15-Nsp16 site
252 (Fig. 3e) had a surprisingly low ASA (542 \AA^2) versus the other SARS-CoV-2 cleavage sites
253 analyzed (mean of others 890 \AA^2 , SD = 102 \AA^2), and as compared to the P5-P4' residues of
254 known substrates of other proteases in the chymotrypsin family (mean 678 \AA^2 , SD = 297 \AA^2)
255 (Additional File 1: Table S11).

256 As previously noted, NetCorona predicted cleavage sites in 22 of the 71 proteins
257 Moustaqil *et al.* studied, but cleavages were only observed *in vitro* in two proteins [46]. Nsp5
258 access scores could be provided for 9 unique motifs from the 22 proteins NetCorona predicted
259 to be cleaved, the mean of which was 332 (SD = 143). The sum of this mean and one standard
260 deviation gives a Nsp5 access score of 475. 30 cleavage sites identified *in vitro* by Koudelka *et*
261 *al.* could be assigned a Nsp5 access score [47], the mean of which was 381 (SD = 150). The
262 sum of this mean and one standard deviation gives a Nsp5 access score of 531.

263 Based on these comparisons to available experimental data, a Nsp5 access score cut-
264 off of 500 was selected, which is further illustrated in Additional File 7: Figure S2 (full data in
265 Additional File 1: Table S12). This cut-off accommodates motifs with marginal NetCorona
266 scores (~0.5) but maximally observed ASA (~ 1000 \AA^2), and the opposite scenario where a low
267 ASA comparable to Nsp15-Nsp16 (~ 500 \AA^2) is matched with a high NetCorona score (~0.9). 92
268 motifs in 92 human proteins were found to have a Nsp5 access score >500 (Fig. 3f), which were
269 forwarded to the next rounds of analysis.

270

271 **Analysis of Tissue Expression and Subcellular Localization of Predicted Cleaved
272 Proteins**

273 Proteins with a Nsp5 access score above 500 were imputed in STRING within the Cytoscape
274 environment [65-67]. The STRING app computes protein network interaction by integrating
275 information from publicly available databases, such as Reactome and Uniprot. Through
276 textmining of the articles reported in those databases, it also compiles scores for multiple
277 tissues and cellular compartment. The nucleus and cytosol were the top locations for human
278 proteins with a highly predicted Nsp5 cleavage site (Fig. 4a), and the highest expression was in
279 the nervous system and liver (Fig. 4b). The mean or summed expression score did not correlate
280 with the Nsp5 access score ($p = 0.03$ and 0.05 respectively), nor was there a correlation
281 between the Nsp5 access score and subcellular localization scores ($p = -0.08$ for mean and -0.17 for sum).

283 Studies of the subcellular localization of coronavirus Nsps provide insight into where
284 Nsp5 may exist in infected cells, and thus what human proteins it may be exposed to. Flanked
285 by transmembrane proteins Nsp4 and Nsp6 in the polyprotein, Nsp5 is exposed to the cytosol
286 when first expressed, where it colocalizes with Nsp3 once released [68-70]. Recent studies
287 have indicated that SARS-CoV-2 Nsp5 activity can be detected throughout the cytosol of a
288 patient's cells *ex vivo* [25], and Nsp5 is also found in the nucleus and ER [51, 71].

289 Through the Human Protein Atlas (HPA), we obtained information on protein expression
290 in tissue by immunohistochemistry (IHC) together with intracellular localization obtained by
291 confocal imaging for most of the proteins in our dataset [72]. Proteins that are not found in the
292 same cellular compartment as Nsp5, or where intracellular localization was unknown, were
293 filtered out. Out of the initial 92 proteins with a Nsp5 access score over 500 and based on
294 current knowledge, only 48 proteins were likely to be found in the same cellular compartment as
295 Nsp5 (Fig. 5, Additional File 1: Table S13-14), indicating the greatest potential for interacting
296 with and being cleaved by the protease. Proteins involved in apoptosis, such as CASP2, E2F1,
297 and FNTA, had both a high Nsp5 access score and an above average expression.

298
299 **Network Analysis and Pathways of Interest**

300 Imputation in STRING of these 48 human proteins with a Nsp5 access score over 500 and
301 plausible colocalization, revealed multiple pathways of interest (Fig. 6, Additional File 1: Table
302 S15). The pathway containing the most proteins that may be targeted by and colocalize with
303 Nsp5 was mRNA processing (DHX15, ELAVL1, LTV1, PABPC3, RPL10, RPUSD1, SKIV2L2,
304 SMG7, TDRD7). Another prominent pathway was apoptosis, with multiple proteins involved

305 directly in apoptosis or its regulation (CASP2, E2F1, FNTA, MAPT, PTPN13). DNA damage
306 response, mediated through ATF2, NEIL1, PARP2, and RAD50 may also be targeted by Nsp5.
307 PARP2 had the second highest Nsp5 access score in our analysis, and the predicted cleavage
308 site at Q352 is located between the DNA-binding domain and the catalytic domain [73].

309 Proteins involved in membrane trafficking (RAB27B and SNX10), or in microtubule
310 organization (DNM1, HTT, MAPRE3, TSC1) were also enriched in this focused dataset, which
311 were grouped together under the descriptor “vesicle trafficking”. Two proteins related to
312 ubiquitination (UBA1 and USP4) were also amongst these potential Nsp5 targets. Nsp3
313 mediated modulation of ubiquitination has been shown to be important for IFN antagonism [32-
314 39], and there is also evidence for Nsp5 mediated reduction of ubiquitination [45, 47]. Finally, a
315 group of proteins implicated in cytokine response was also strongly predicted to be cleaved
316 (AIMP1, MAPK12, and PTPN2), which are involved in downstream signaling of multiple
317 cytokines [74-77].

318

319

320 **Discussion**

321 To provide context to the growing list of coronavirus-host protein-protein interactions, and to aid
322 in the interpretation of experiments focused on human proteins cleaved by coronavirus Nsp5,
323 we applied a bioinformatics approach to predict human proteins cleaved by Nsp5. Our
324 proteome-wide investigation complements *in vitro* experiments, which are limited to only a
325 subset of potential human protein substrates based on what proteins are expressed by the cell
326 type chosen, resulting in different proteins appearing to be cleaved by [47, 48], or interact with
327 Nsp5 [49-54].

328 The NetCorona neural network generated long lists of potentially cleaved human
329 proteins, but mismatches between these predictions and the *in vitro* mapping of Nsp5 cleavage
330 sites indicated that NetCorona scores alone were insufficient for accurate predictions. Similar to
331 previous reports [58-60], solvent accessibility helped to filter predictions based on primary
332 sequence alone, which was made possible thanks to the PSAIA tool which automated the
333 measurement of motif ASA with an easy-to-use GUI that handled batch input of PDB files [64].

334 Human proteins predicted to be cleaved by Nsp5 did not correlate with Nsp5-human
335 protein-protein interactions identified *in vitro*, and Nsp5 overall appears to interact with fewer
336 human proteins compared to other Nsp5s and structural proteins [51]. This may be because the
337 proteolytic activity of Nsp5 reduces the efficiency of proximity labeling/affinity purification,

338 whereby Nsp5 may cleave proteins it interacts with most favorably, reducing the appearance of
339 host protein interactions. The small but statistically significant negative correlation between the
340 strength of the Nsp5-human protein interaction and the human protein's maximum NetCorona
341 score may be evidence of this. Indeed, different sets of interacting proteins are obtained when
342 using the catalytically inactive Nsp5 mutant C145A versus the wildtype Nsp5 [49, 51, 54]. We
343 therefore hypothesize that the interactions observed by proximity labeling/affinity purification do
344 not reflect Nsp5 mediated proteolysis and instead represent non-proteolytic protein-protein
345 interactions, which may still be important to understanding Nsp5's role in modulating host
346 protein networks.

347 N-terminomics based approaches have identified many potential Nsp5 cleavage sites in
348 human proteins [47, 48], but they have some limitations that bioinformatics can compliment.
349 Trypsin is used in the preparation of samples for mass spectrometry, which generates
350 cleavages at lysine and arginine residues that are not N-terminal to a proline. Lysine and
351 arginine appear in many cleavage sites predicted by NetCorona, meaning that cleavage by
352 trypsin may mask true cleavage sites by artificially generating a N-terminus proximal to a P1
353 glutamine residue. Only one protein overlaps between the Koudelka *et al.* and Meyer *et al.*
354 results, as these studies used different cell lines, and thus different proteins will be expressed,
355 and the methods of exposure to Nsp5 also differed (cell lysate incubated with Nsp5 vs SARS-
356 CoV-2 infection of cells) [47, 48]. Meyer *et al.* point out that the lysate-based method used by
357 Koudelka *et al.* strips proteins of their subcellular context, which may lead to observed cleavage
358 events that are not possible *in vivo* during infection [48]. In contrast, our bioinformatics analysis
359 is cell-type and methodology agnostic as it examined the entire human proteome. The cleavage
360 sites predicted *in silico*, combined with knowledge of Nsp5 subcellular localization and protein
361 networks, identified several interesting human proteins and pathways.

362 DHX15 contained a predicted cleavage site with the highest Nsp5 access score, and the
363 protein may co-localize with Nsp5 in the nuclei of infected cells, making it a significant protein of
364 interest. DHX15 is a DExD/H-box helicase, a family of proteins that serves to detect foreign
365 RNA, triggering an antiviral response (reviewed by [78]). The role of DHX15 in anti-viral defense
366 is diverse, including by binding viral RNA with NLRP6, which activates Type I/III interferons and
367 IFN-stimulated genes in the intestine of mice [79]. DHX15 mediated sensing of viral RNA
368 activates MAPK and NK- κ B innate immune signaling [80], and also acts as a coreceptor of viral
369 RNA with RIG-I that increases antiviral response and cytokine production [81].

370 DHX15 is not reported to be a significant interactor with SARS-CoV-2 proteins [51],
371 however it is capable of binding both dsRNA and ssRNA [81], suggesting it could bind

372 coronavirus ssRNA. The location of the predicted Nsp5 cleavage site (Q788) is very close to its
373 C-terminus (Y795), so cleavage by Nsp5 would remove only seven amino acids. However, there
374 is a SUMOylation site (K786) at P3 of the cleavage motif, and the de-SUMOylation of DHX15
375 results in increased antiviral signaling [82]. Therefore, it is possible that Nsp5 cleavage at Q788
376 may disrupt SUMOylation, by reducing the length of the peptide accessible by the SUMOylation
377 complex, contributing to the general dysregulation of a coordinated innate immune response to
378 viral infection.

379 PARP2 contained a predicted Nsp5 cleavage site with the second highest Nsp5 access
380 score, at Q352. PARP2 is involved in DNA damage recognition and repair, and its correct
381 functioning prevents apoptosis in the event of a double stranded break (DSB) [83]. PARP2 also
382 plays a role in the adaptive immune system, as it helps prevent the accumulation of DSBs
383 during TCR α gene rearrangements in thymocytes, promoting T-cell maturation [84]. The
384 predicted Nsp5 site occurs between the DNA binding and catalytic domains of PARP2 [85],
385 meaning the cleaved protein would be unable to recognize damaged DNA, contributing to
386 apoptosis. Interestingly, this is similar to the native activity of human caspase-8, which cleaves
387 PARP2 in its DNA binding domain during apoptosis [86]. SARS-CoV-2 infection of lung
388 epithelial cells was found to increase caspase-8 activity, resulting in cleaved PARP1, a homolog
389 of PARP2 [87]. SARS-CoV Nsp5 activity is known to be pro-apoptotic, via the activation of
390 caspase-3 and caspase-9 [88]. Overall, if coronavirus Nsp5 cleaves PARP2, it could contribute
391 to the pro-apoptotic cell state observed in infected cells.

392 Proteins with roles in cytokine response and antiviral defense were also identified as
393 strongly predicted targets of Nsp5 cleavage (AIMP1, MAPK12, PTPN2). AIMP1 is crucial to
394 antiviral defense in mice [74], and it is targeted for degradation by hepatitis C virus envelope
395 protein E2 [75]. MAPK12 function appears to be important for SARS-CoV-2 replication, as
396 knockdown by siRNA results in lower virus titers [76]. This phenotype is similar to the
397 knockdown of Nsp5 targeted proteins resulting in lower virus replication, as observed by Meyer
398 *et al.* [48]. T-cell protein tyrosine phosphatase, PTPN2, negatively regulates the antiviral
399 response of MITA [89] and the JAK-STAT pathway of the innate immune system [90]. Knockout
400 of PTPN2 results in systemic inflammatory responses in mice resulting in premature death [91],
401 and a genetic polymorphism resulting in PTPN2 loss of function increases ACE2 expression,
402 resulting in greater susceptibility to SARS-CoV-2 infection [77].

403 The modulation of mRNA processing, DNA damage recognition/apoptosis, and cytokine
404 signaling stood out as the most interesting pathways that may be influenced by Nsp5 cleavage.
405 As coronaviruses are known to bias mRNA processing, trigger apoptosis, and disrupt innate

406 immune responses (reviewed by [15]), these results suggest that Nsp5 mediated cleavage may
407 aid in the molecular pathogenesis of diseases caused by coronaviruses diseases. These
408 pathways, and specific proteins mentioned above, represent interesting targets for further
409 analysis *in vitro*.

410

411

412 **Limitations**

413 Recent studies comparing Nsp5 proteases from various coronaviruses have indicated that
414 despite sharing significant sequence and structural similarity, they cleave and interact with
415 different human proteins *in vitro* [47, 54]. In general, a pan-coronavirus predictor of Nsp5
416 cleavage sites may not be feasible. For example, SARS-CoV-2 Nsp5 accommodates more
417 diversity at P2 than SARS-CoV Nsp5 [25], which would influence the human proteins that could
418 be cleaved. Refinements to the NetCorona neural network to improve its predictive accuracy, or
419 make them virus-specific, would be beneficial and have recently been attempted [92]. Nsp5 also
420 likely accommodates more diversity at P1' and P3 than what NetCorona was trained on, based
421 on the naturally occurring 1ab variants we report here, and the human proteins observed to be
422 cleaved *in vitro*. That histidine can be accommodated at P1 and phenylalanine at P2, albeit
423 unfavorably, further adds complexity to what human proteins may be cleaved by Nsp5 [17, 25,
424 47, 61]. The results of this study are instead meant to provide guidance for *in vitro* experimental
425 design and interpretation of experimental results, in addition to suggesting proteome-wide
426 trends in molecular pathways that Nsp5 mediated cleavage may disrupt.

427

428

429 **Conclusions**

430 The large volume of recent coronavirus research and data requires proteome-wide views of
431 interpretation. The results of this study are intended to compliment the various *in vitro*
432 approaches that have been used to identify Nsp5-human protein interactions, and to map
433 specific Nsp5 cleavage sites in human proteins. As Meyer *et al.* discuss, specific targeting of
434 proteins by Nsp5 appears likely, as the knockdown of certain Nsp5-targeted proteins reduces
435 viral reproduction [48]. We have built upon the original NetCorona study by performing detailed
436 structural analysis of predicted cleavage sites, and protein network and pathway analysis.
437 Coronavirus Nsp5 was predicted to play a role in the targeted disruption of mRNA processing,

438 cytokine response, and apoptosis, which are interesting targets for future analysis and
439 characterization. We hope that our analysis and the proteome-wide datasets generated will aid
440 in the interpretation and design of additional experiments towards understanding Nsp5's role in
441 coronavirus molecular pathology.

442

443

444 **Methods**

445 **Amino Acid Sequence Datasets**

446 Three datasets of amino acid sequences of human proteins were downloaded from the UniProt
447 reference human proteome on April 14 2020: "All Human Proteins" contains 74811 human
448 protein sequences including splice variants and predicted proteins; "One Protein Per Gene"
449 contains 20595 human protein sequences where only one sequence is provided for each gene;
450 "Proteins With PDB" is the "All Human Proteins" dataset filtered in UniProt for associated entries
451 in the RCSB Protein Data Bank, generating a dataset of 6806 human protein sequences. 9404
452 amino acid sequences of the SARS-CoV-2 1ab polyprotein were obtained from NCBI Virus on
453 August 4 2020. Sequences with inconclusive "X" residues were filtered out as they were not
454 correctly handled by NetCorona, leaving 8017 SARS-CoV-2 1ab polyprotein sequences to be
455 analyzed.

456

457 **NetCorona Analysis**

458 The command line version of NetCorona was used to predict Nsp5 cleavage site scores for
459 human and viral protein sequences [55]. To overcome the input file limit of 50,000 amino acids
460 per submission and handle sequences with non-standard amino acids, a Python script was
461 developed. This script partitions the input data, runs the NetCorona neural network on each
462 subset, and parses and concatenates the output data. The output file includes sequence
463 accession number, position of P1-Glutamine (Q) residue, Netcorona score (0.000-1.000) and a
464 10 amino acid sequence motif of positions P5-P5' (Additional File 2-4). Note that the neural
465 network itself uses positions P5-P4' (9 residues) for calculating the score. Gene names and
466 other identifiers associated with each UniProt ID containing a NetCorona score >0.5 were
467 collected in Microsoft Excel (Additional File 1: Table S2-S4). Scores from NetCorona run on
468 each dataset of proteins were parsed and compared with a Kolmogorov-Smirnov (KS) test, to
469 assess the null hypothesis that the scores for each population are drawn from the same
470 distribution. Unique glutamine motifs from 1ab polyprotein sequences were identified using

471 Microsoft Excel (Additional File 1: Table S1). Statistical analysis and the generation of graphs
472 was performed using GraphPad Prism (version 9.1.0)

473

474 **Structural Analysis**

475 PDB metadata associated with proteins in the “Proteins With PDB” dataset that also contained a
476 predicted Nsp5 cleavage (NetCorona score >0.5), were downloaded from the RCSB PDB
477 website by generating a custom report in .csv format. Homology models, and structures with a
478 resolution greater than 8Å or where resolution was not reported, were removed. Nsp5 cleavage
479 sites predicted by NetCorona were matched with one PDB file per cleavage site, by searching
480 the PDB metadata for the predicted 9 amino acid cleavage motif using Microsoft Excel
481 (Additional File 6). The entire predicted 9 amino acid motif must appear in the PDB file to be
482 considered a match. Matches between a PDB file and predicted cleavage motif were manually
483 corrected when the motif sequence appeared by chance in a PDB containing the incorrect
484 protein.

485 PDB files containing a predicted Nsp5 cleavage site were then batch downloaded from
486 the RCSB PDB, and analyzed 100 at a time using the Protein Structure and Interaction Analyzer
487 (PSAIA) tool using default settings [64], with chains in each PDB analyzed independently. The
488 total accessible surface area (ASA) of each residue was calculated using a Z slice of 0.25 Å and
489 a probe radius of 1.4 Å. XML files output by PSAIA were combined in Microsoft Excel, to create
490 searchable datasets for each 9 amino acid motif predicted to be cleaved by NetCorona, and the
491 total ASA of all atoms in each 9 amino acid motif were summed. The motif’s ASA was then
492 multiplied by the NetCorona score to provide a Nsp5 access score.

493 Proteins known to be cleaved by mammalian chymotrypsin-like proteases were
494 independently obtained from the RCSB PDB, and the known cleaved motifs were analyzed as
495 above. Protein structures and homology models of SARS-CoV-2 proteins were obtained the
496 RCSB PDB and from SWISS-MODEL [93] and were analyzed as above. Publication quality
497 figures were generated using PyMOL 2.3.0.

498

499 **Tissue Expression and Subcellular Localization Analysis**

500 Proteins with Nsp5 access score above 500 were loaded into the STRING app [65] within
501 Cytoscape [66] (version 1.6.0 and 3.8.2 respectively) using Uniprot ID, Homo sapiens
502 background, 0.80 confidence score cut-off and no additional interactor for the pathway
503 enrichment analysis (Additional File 1: Table S13-S15). The node table (including tissue

504 expression scores and compartments score for each protein) was exported to R for wrangling
505 and data visualization using the tidyverse and ggrepel packages [94-96].

506 To increase confidence, tissue expression and subcellular localization data were
507 obtained from the Human Protein Atlas which are all based on immunohistochemistry (tissue
508 expression) or confocal microscopy (subcellular localization) [72, 97]. Each entry was then
509 matched in R, table joining was done using Uniprot IDs. Expression levels noted as “Not
510 detected”, “Low”, “Medium” or “High” were replaced by numeric values ranging from 0 to 3.
511 Mean expression was calculated as the mean expression across all tissues, removing missing
512 values from the analysis.

513 The following intracellular locations were used to encompass the nucleus, cytoplasm
514 and endoplasmic reticulum: "Cytosol", "Nucleoplasm", "Endoplasmic reticulum", "Microtubules",
515 "Nuclear speckles", "Intermediate filaments", "Nucleoli", "Nuclear bodies". All the proteins that
516 did not include one or more of these locations in the HPA database were excluded from further
517 analysis.

518

519 **Protein Network Analysis**

520 The 48 proteins with a Nsp5 access score >500 and that had the potential to be found in the
521 same cellular compartment as Nsp5 were imported into the STRING app (again within
522 Cytoscape) while allowing a maximum of 5 additional interactor for the network generation
523 instead of none. All the other parameters were left unchanged. Individual nodes that had no
524 protein-protein interactions with other proteins in the network were manually moved closer to
525 other nodes presenting the same or similar pathway. When proteins could interact in multiple
526 pathways represented here, a “main pathway” was assigned based on literature search. Node
527 color was a gradient based on Nsp5 access score. Node size increased with the mean
528 expression. Edges represent protein-protein interaction (confidence > 0.80). Gene name labels
529 were colored based on the Nsp5 access score for readability only.

530

531

532 **Acknowledgements**

533 We wish to thank the Crowdfight COVID (crowdfightcovid19.org) for facilitating this collaboration, and Ian M. Boyce
534 for assistance editing figures. The National Institute of Standards and Technology (NIST) notes that certain software
535 and materials are identified in this article to explain a procedure as completely as possible. This does not imply a
536 recommendation or endorsement by NIST, nor does it imply that the particular materials are necessarily the best
537 available for the purpose. The opinions expressed in this article are the authors' own and do not necessarily
538 represent the views of NIST.

539

540 Author Contributions

541 BMS conceived the idea and supervised the study. BMS, VL, DGB, NSB generated the data. BMS, VL, PDT
542 analyzed the data. BMS, VL, DGB generated the figures. BMS and VL drafted the manuscript. All authors edited the
543 manuscript. BMS acted as corresponding author. All the authors have read and approved the final manuscript.

544

545 Funding

546 BMS is an International Associate of NIST, supported through the Professional Research Experience Program
547 agreement with the University of Maryland. PDT was supported by a National Research Council Postdoctoral
548 Research Associateship. This study was not funded by any specific grant.

549

550 Availability of Data and Materials

551 PSAIA was obtained here: <http://complex.zesoi.fer.hr/index.php/en/10-category-en-gb/tools-en/19-psaia-en>

552

553 References

1. Andersen KG, Rambaut A, Lipkin WI, Holmes EC, Garry RF: **The proximal origin of SARS-CoV-2.** *Nat Med* 2020, **26**(4):450-452.
2. Zhou H, Chen X, Hu T, Li J, Song H, Liu Y, Wang P, Liu D, Yang J, Holmes EC *et al*: **A Novel Bat Coronavirus Closely Related to SARS-CoV-2 Contains Natural Insertions at the S1/S2 Cleavage Site of the Spike Protein.** *Curr Biol* 2020, **30**(11):2196-2203 e2193.
3. Wilder-Smith A, Chiew CJ, Lee VJ: **Can we contain the COVID-19 outbreak with the same measures as for SARS?** *Lancet Infect Dis* 2020, **20**(5):e102-e107.
4. Petersen E, Koopmans M, Go U, Hamer DH, Petrosillo N, Castelli F, Storgaard M, Al Khalili S, Simonsen L: **Comparing SARS-CoV-2 with SARS-CoV and influenza pandemics.** *Lancet Infect Dis* 2020, **20**(9):e238-e244.
5. Yang X, Yu Y, Xu J, Shu H, Xia J, Liu H, Wu Y, Zhang L, Yu Z, Fang M *et al*: **Clinical course and outcomes of critically ill patients with SARS-CoV-2 pneumonia in Wuhan, China: a single-centered, retrospective, observational study.** *Lancet Respir Med* 2020, **8**(5):475-481.
6. Robba C, Battaglini D, Pelosi P, Rocco PRM: **Multiple organ dysfunction in SARS-CoV-2: MODS-CoV-2.** *Expert Rev Respir Med* 2020:1-4.
7. Puelles VG, Lutgehetmann M, Lindenmeyer MT, Sperhake JP, Wong MN, Allweiss L, Chilla S, Heinemann A, Wanner N, Liu S *et al*: **Multiorgan and Renal Tropism of SARS-CoV-2.** *N Engl J Med* 2020.
8. Helms J, Tacquare C, Severac F, Leonard-Lorant I, Ohana M, Delabranche X, Merdji H, Clere-Jehl R, Schenck M, Fagot Gonet F *et al*: **High risk of thrombosis in patients with severe SARS-CoV-2 infection: a multicenter prospective cohort study.** *Intensive Care Med* 2020, **46**(6):1089-1098.
9. Xu L, Liu J, Lu M, Yang D, Zheng X: **Liver injury during highly pathogenic human coronavirus infections.** *Liver Int* 2020, **40**(5):998-1004.
10. Whittaker A, Anson M, Harky A: **Neurological Manifestations of COVID-19: A systematic review and current update.** *Acta Neurol Scand* 2020, **142**(1):14-22.
11. Giamarellos-Bourboulis EJ, Netea MG, Rovina N, Akinosoglou K, Antoniadou A, Antonakos N, Damoraki G, Gkavogianni T, Adami ME, Katsaounou P *et al*: **Complex Immune Dysregulation in COVID-19 Patients with Severe Respiratory Failure.** *Cell Host Microbe* 2020, **27**(6):992-1000 e1003.
12. Lucas C, Wong P, Klein J, Castro TBR, Silva J, Sundaram M, Ellingson MK, Mao T, Oh JE, Israelow B *et al*: **Longitudinal analyses reveal immunological misfiring in severe COVID-19.** *Nature* 2020, **584**(7821):463-469.
13. Kuri-Cervantes L, Pampena MB, Meng W, Rosenfeld AM, Ittner CAG, Weisman AR, Agyekum RS, Mathew D, Baxter AE, Vella LA *et al*: **Comprehensive mapping of immune perturbations associated with severe COVID-19.** *Sci Immunol* 2020, **5**(49).
14. Mathew D, Giles JR, Baxter AE, Oldridge DA, Greenplate AR, Wu JE, Alanio C, Kuri-Cervantes L, Pampena MB, D'Andrea K *et al*: **Deep immune profiling of COVID-19 patients reveals distinct immunotypes with therapeutic implications.** *Science* 2020, **369**(6508).
15. Hartenian E, Nandakumar D, Lari A, Ly M, Tucker JM, Glaunsinger BA: **The molecular virology of coronaviruses.** *J Biol Chem* 2020, **295**(37):12910-12934.

592 16. Ziebuhr J, Snijder EJ, Gorbalyena AE: **Virus-encoded proteinases and proteolytic processing in the**
593 **Nidovirales**. *J Gen Virol* 2000, **81**(Pt 4):853-879.

594 17. Chuck CP, Chow HF, Wan DC, Wong KB: **Profiling of substrate specificities of 3C-like proteases from**
595 **group 1, 2a, 2b, and 3 coronaviruses**. *PLoS One* 2011, **6**(11):e27228.

596 18. Ullrich S, Nitsche C: **The SARS-CoV-2 main protease as drug target**. *Bioorg Med Chem Lett* 2020,
597 **30**(17):127377.

598 19. Hegyi A, Ziebuhr J: **Conservation of substrate specificities among coronavirus main proteases**. *J Gen*
599 *Virol* 2002, **83**(Pt 3):595-599.

600 20. Tomar S, Johnston ML, St John SE, Osswald HL, Nyalapatala PR, Paul LN, Ghosh AK, Denison MR,
601 Mesecar AD: **Ligand-induced Dimerization of Middle East Respiratory Syndrome (MERS) Coronavirus**
602 **nsp5 Protease (3CLpro): IMPLICATIONS FOR nsp5 REGULATION AND THE DEVELOPMENT OF**
603 **ANTIVIRALS**. *J Biol Chem* 2015, **290**(32):19403-19422.

604 21. Muramatsu T, Kim YT, Nishii W, Terada T, Shirouzu M, Yokoyama S: **Autoprocessing mechanism of**
605 **severe acute respiratory syndrome coronavirus 3C-like protease (SARS-CoV 3CLpro) from its**
606 **polyproteins**. *FEBS J* 2013, **280**(9):2002-2013.

607 22. Zhang L, Lin D, Sun X, Curth U, Drosten C, Sauerhering L, Becker S, Rox K, Hilgenfeld R: **Crystal**
608 **structure of SARS-CoV-2 main protease provides a basis for design of improved alpha-ketoamide**
609 **inhibitors**. *Science* 2020, **368**(6489):409-412.

610 23. Jin Z, Du X, Xu Y, Deng Y, Liu M, Zhao Y, Zhang B, Li X, Zhang L, Peng C *et al*: **Structure of M(pro) from**
611 **SARS-CoV-2 and discovery of its inhibitors**. *Nature* 2020, **582**(7811):289-293.

612 24. Yoshimoto FK: **The Proteins of Severe Acute Respiratory Syndrome Coronavirus-2 (SARS CoV-2 or n-**
613 **COV19), the Cause of COVID-19**. *Protein J* 2020, **39**(3):198-216.

614 25. Rut W, Groborz K, Zhang L, Sun X, Zmudzinski M, Pawlik B, Wang X, Jochmans D, Neyts J, Mlynarski W *et*
615 *al*: **SARS-CoV-2 M(pro) inhibitors and activity-based probes for patient-sample imaging**. *Nat Chem*
616 *Biol* 2021, **17**(2):222-228.

617 26. Angelini MM, Akhlaghpour M, Neuman BW, Buchmeier MJ: **Severe acute respiratory syndrome**
618 **coronavirus nonstructural proteins 3, 4, and 6 induce double-membrane vesicles**. *mBio* 2013, **4**(4).

619 27. Wolff G, Limpens R, Zevenhoven-Dobbe JC, Laugks U, Zheng S, de Jong AWM, Koning RI, Agard DA,
620 Grunewald K, Koster AJ *et al*: **A molecular pore spans the double membrane of the coronavirus**
621 **replication organelle**. *Science* 2020, **369**(6509):1395-1398.

622 28. Totura AL, Baric RS: **SARS coronavirus pathogenesis: host innate immune responses and viral**
623 **antagonism of interferon**. *Curr Opin Virol* 2012, **2**(3):264-275.

624 29. Lei J, Hilgenfeld R: **RNA-virus proteases counteracting host innate immunity**. *FEBS Lett* 2017,
625 **591**(20):3190-3210.

626 30. de Wilde AH, Snijder EJ, Kikkert M, van Hemert MJ: **Host Factors in Coronavirus Replication**. *Curr Top*
627 *Microbiol Immunol* 2018, **419**:1-42.

628 31. Lei X, Dong X, Ma R, Wang W, Xiao X, Tian Z, Wang C, Wang Y, Li L, Ren L *et al*: **Activation and evasion**
629 **of type I interferon responses by SARS-CoV-2**. *Nature communications* 2020, **11**(1):3810.

630 32. Shin D, Mukherjee R, Grawe D, Bojkova D, Baek K, Bhattacharya A, Schulz L, Widera M, Mehdipour AR,
631 Tascher G *et al*: **Papain-like protease regulates SARS-CoV-2 viral spread and innate immunity**. *Nature*
632 2020, **587**(7835):657-662.

633 33. Frieman M, Ratia K, Johnston RE, Mesecar AD, Baric RS: **Severe acute respiratory syndrome**
634 **coronavirus papain-like protease ubiquitin-like domain and catalytic domain regulate antagonism of**
635 **IRF3 and NF-kappaB signaling**. *J Virol* 2009, **83**(13):6689-6705.

636 34. Yang X, Chen X, Bian G, Tu J, Xing Y, Wang Y, Chen Z: **Proteolytic processing, deubiquitinase and**
637 **interferon antagonist activities of Middle East respiratory syndrome coronavirus papain-like**
638 **protease**. *J Gen Virol* 2014, **95**(Pt 3):614-626.

639 35. Mielech AM, Kilianski A, Baez-Santos YM, Mesecar AD, Baker SC: **MERS-CoV papain-like protease has**
640 **deISGylating and deubiquitinating activities**. *Virology* 2014, **450-451**:64-70.

641 36. Chen X, Yang X, Zheng Y, Yang Y, Xing Y, Chen Z: **SARS coronavirus papain-like protease inhibits the**
642 **type I interferon signaling pathway through interaction with the STING-TRAF3-TBK1 complex**. *Protein*
643 *Cell* 2014, **5**(5):369-381.

644 37. Li SW, Wang CY, Jou YJ, Huang SH, Hsiao LH, Wan L, Lin YJ, Kung SH, Lin CW: **SARS Coronavirus**
645 **Papain-Like Protease Inhibits the TLR7 Signaling Pathway through Removing Lys63-Linked**
646 **Polyubiquitination of TRAF3 and TRAF6**. *Int J Mol Sci* 2016, **17**(5).

647 38. Knaap RCM, Fernández-Delgado R, Dalebout TJ, Oreshkova N, Bredenbeek PJ, Enjuanes L, Sola I, Snijder
648 EJ, Kikkert M: **The deubiquitinating activity of Middle East respiratory syndrome coronavirus papain-**
649 **like protease delays the innate immune response and enhances virulence in a mouse model**. *bioRxiv*
650 2019:751578.

651 39. Freitas BT, Durie IA, Murray J, Longo JE, Miller HC, Crich D, Hogan RJ, Tripp RA, Pegan SD:
652 **Characterization and Noncovalent Inhibition of the Deubiquitinase and deISGylase Activity of SARS-**
653 **CoV-2 Papain-Like Protease**. *ACS Infect Dis* 2020, **6**(8):2099-2109.

654 40. Wang D, Fang L, Shi Y, Zhang H, Gao L, Peng G, Chen H, Li K, Xiao S: **Porcine Epidemic Diarrhea Virus**
655 **3C-Like Protease Regulates Its Interferon Antagonism by Cleaving NEMO**. *J Virol* 2016, **90**(4):2090-
656 2101.

657 41. Zhu X, Fang L, Wang D, Yang Y, Chen J, Ye X, Foda MF, Xiao S: **Porcine deltacoronavirus nsp5 inhibits**
658 **interferon-beta production through the cleavage of NEMO**. *Virology* 2017, **502**:33-38.

659 42. Chen S, Tian J, Li Z, Kang H, Zhang J, Huang J, Yin H, Hu X, Qu L: **Feline Infectious Peritonitis Virus**
660 **Nsp5 Inhibits Type I Interferon Production by Cleaving NEMO at Multiple Sites**. *Viruses* 2019, **12**(1).

661 43. Zhu X, Wang D, Zhou J, Pan T, Chen J, Yang Y, Lv M, Ye X, Peng G, Fang L *et al*: **Porcine**
662 **Deltacoronavirus nsp5 Antagonizes Type I Interferon Signaling by Cleaving STAT2**. *J Virol* 2017,
663 **91**(10).

664 44. Xia H, Cao Z, Xie X, Zhang X, Chen JY, Wang H, Menachery VD, Rajsbaum R, Shi PY: **Evasion of Type I**
665 **Interferon by SARS-CoV-2**. *Cell Rep* 2020:108234.

666 45. Wu Y, Ma L, Zhuang Z, Cai S, Zhao Z, Zhou L, Zhang J, Wang P-H, Zhao J, Cui J: **Main protease of**
667 **SARS-CoV-2 serves as a bifunctional molecule in restricting type I interferon antiviral signaling**.
668 *Signal Transduction and Targeted Therapy* 2020, **5**(1):221.

669 46. Mousaqil M, Ollivier E, Chiu HP, Van Tol S, Rudolffi-Soto P, Stevens C, Bhumkar A, Hunter DJB, Freiberg
670 AN, Jacques D *et al*: **SARS-CoV-2 proteases PLpro and 3CLpro cleave IRF3 and critical modulators of**
671 **inflammatory pathways (NLRP12 and TAB1): implications for disease presentation across species**.
672 *Emerg Microbes Infect* 2021, **10**(1):178-195.

673 47. Koudelka T, Boger J, Henkel A, Schonherr R, Krantz S, Fuchs S, Rodriguez E, Redecke L, Tholey A: **N-**
674 **Terminomics for the Identification of In Vitro Substrates and Cleavage Site Specificity of the SARS-**
675 **CoV-2 Main Protease**. *Proteomics* 2021, **21**(2):e2000246.

676 48. Meyer B, Chiaravalli J, Gellenoncourt S, Brownridge P, Bryne DP, Daly LA, Walter M, Agou F, Chakrabarti
677 LA, Craik CS *et al*: **Characterisation of protease activity during SARS-CoV-2 infection identifies novel**
678 **viral cleavage sites and cellular targets for drug repurposing**. *bioRxiv* 2021:2020.2009.2016.297945.

679 49. Gordon DE, Jang GM, Bouhaddou M, Xu J, Obernier K, White KM, O'Meara MJ, Rezelj VV, Guo JZ,
680 Swaney DL *et al*: **A SARS-CoV-2 protein interaction map reveals targets for drug repurposing**. *Nature*
681 2020, **583**(7816):459-468.

682 50. Bojkova D, Klann K, Koch B, Widera M, Krause D, Ciesek S, Cinatl J, Munch C: **Proteomics of SARS-CoV-**
683 **2-infected host cells reveals therapy targets**. *Nature* 2020, **583**(7816):469-472.

684 51. Samavarchi-Tehrani P, Abdouni H, Knight JDR, Astori A, Samson R, Lin Z-Y, Kim D-K, Knapp JJ, St-
685 Germain J, Go CD *et al*: **A SARS-CoV-2 – host proximity interactome**. *bioRxiv*
686 2020:2020.2009.2003.282103.

687 52. Laurent EMN, Sofianatos Y, Komarova A, Gimeno J-P, Tehrani PS, Kim D-K, Abdouni H, Duhamel M,
688 Cassonnet P, Knapp JJ *et al*: **Global BioID-based SARS-CoV-2 proteins proximal interactome unveils**
689 **novel ties between viral polypeptides and host factors involved in multiple COVID19-associated**
690 **mechanisms**. *bioRxiv* 2020:2020.2008.2028.272955.

691 53. Li J, Guo M, Tian X, Wang X, Yang X, Wu P, Liu C, Xiao Z, Qu Y, Yin Y *et al*: **Virus-Host Interactome and**
692 **Proteomic Survey Reveal Potential Virulence Factors Influencing SARS-CoV-2 Pathogenesis**. *Med (N*
693 *Y)* 2021, **2**(1):99-112 e117.

694 54. Gordon DE, Hiatt J, Bouhaddou M, Rezelj VV, Ulferts S, Braberg H, Jureka AS, Obernier K, Guo JZ, Batra J
695 *et al*: **Comparative host-coronavirus protein interaction networks reveal pan-viral disease**
696 **mechanisms**. *Science* 2020, **370**(6521).

697 55. Kiemer L, Lund O, Brunak S, Blom N: **Coronavirus 3CLpro proteinase cleavage sites: possible**
698 **relevance to SARS virus pathology**. *BMC Bioinformatics* 2004, **5**:72.

699 56. Hubbard SJ, Campbell SF, Thornton JM: **Molecular recognition. Conformational analysis of limited**
700 **proteolytic sites and serine proteinase protein inhibitors**. *J Mol Biol* 1991, **220**(2):507-530.

701 57. Kazanov MD, Igarashi Y, Eroshkin AM, Cieplak P, Ratnikov B, Zhang Y, Li Z, Godzik A, Osterman AL, Smith
702 JW: **Structural determinants of limited proteolysis**. *J Proteome Res* 2011, **10**(8):3642-3651.

703 58. Boyd SE, Pike RN, Rudy GB, Whisstock JC, Garcia de la Banda M: **PoPS: a computational tool for**
704 **modeling and predicting protease specificity**. *J Bioinform Comput Biol* 2005, **3**(3):551-585.

705 59. Verspurten J, Gevaert K, Declercq W, Vandenebeele P: **SitePredicting the cleavage of proteinase**
706 **substrates**. *Trends Biochem Sci* 2009, **34**(7):319-323.

707 60. Song J, Tan H, Perry AJ, Akutsu T, Webb GI, Whisstock JC, Pike RN: **PROSPER: an integrated feature-**
708 **based tool for predicting protease substrate cleavage sites**. *PLoS One* 2012, **7**(11):e50300.

709 61. Muramatsu T, Takemoto C, Kim YT, Wang H, Nishii W, Terada T, Shirouzu M, Yokoyama S: **SARS-CoV**
710 **3CL protease cleaves its C-terminal autoprocessing site by novel subsite cooperativity**. *Proc Natl*
711 *Acad Sci U S A* 2016, **113**(46):12997-13002.

712 62. Peng K, Obradovic Z, Vucetic S: **Exploring bias in the Protein Data Bank using contrast classifiers**. *Pac*
713 *Symp Biocomput* 2004:435-446.

714 63. Lee B, Richards FM: **The interpretation of protein structures: estimation of static accessibility**. *J Mol*
715 *Biol* 1971, **55**(3):379-400.

716 64. Mihel J, Sikic M, Tomic S, Jeren B, Vlahovicek K: **PSAIA - protein structure and interaction analyzer.**
717 *BMC Struct Biol* 2008, **8**:21.

718 65. Doncheva NT, Morris JH, Gorodkin J, Jensen LJ: **Cytoscape StringApp: Network Analysis and**
719 **Visualization of Proteomics Data.** *J Proteome Res* 2019, **18**(2):623-632.

720 66. Shannon P, Markiel A, Ozier O, Baliga NS, Wang JT, Ramage D, Amin N, Schwikowski B, Ideker T:
721 **Cytoscape: a software environment for integrated models of biomolecular interaction networks.**
722 *Genome Res* 2003, **13**(11):2498-2504.

723 67. Su G, Morris JH, Demchak B, Bader GD: **Biological network exploration with Cytoscape 3.** *Curr Protoc*
724 *Bioinformatics* 2014, **47**:8 13 11-24.

725 68. Oostra M, Hagemeyer MC, van Gent M, Bekker CP, te Lintel EG, Rottier PJ, de Haan CA: **Topology and**
726 **membrane anchoring of the coronavirus replication complex: not all hydrophobic domains of nsp3**
727 **and nsp6 are membrane spanning.** *J Virol* 2008, **82**(24):12392-12405.

728 69. Snijder EJ, van der Meer Y, Zevenhoven-Dobbe J, Onderwater JJ, van der Meulen J, Koerten HK,
729 Mommaas AM: **Ultrastructure and origin of membrane vesicles associated with the severe acute**
730 **respiratory syndrome coronavirus replication complex.** *J Virol* 2006, **80**(12):5927-5940.

731 70. Knoops K, Kikkert M, Worm SH, Zevenhoven-Dobbe JC, van der Meer Y, Koster AJ, Mommaas AM, Snijder
732 EJ: **SARS-coronavirus replication is supported by a reticulovesicular network of modified**
733 **endoplasmic reticulum.** *PLoS Biol* 2008, **6**(9):e226.

734 71. Zhang J, Cruz-Cosme R, Zhuang MW, Liu D, Liu Y, Teng S, Wang PH, Tang Q: **A systemic and molecular**
735 **study of subcellular localization of SARS-CoV-2 proteins.** *Signal Transduct Target Ther* 2020, **5**(1):269.

736 72. Thul PJ, Akesson L, Wiking M, Mahdessian D, Geladaki A, Ait Blal H, Alm T, Asplund A, Bjork L, Breckels
737 LM *et al:* **A subcellular map of the human proteome.** *Science* 2017, **356**(6340).

738 73. Riccio AA, Cingolani G, Pascal JM: **PARP-2 domain requirements for DNA damage-dependent**
739 **activation and localization to sites of DNA damage.** *Nucleic Acids Res* 2016, **44**(4):1691-1702.

740 74. Liang D, Tian L, You R, Halpert MM, Konduri V, Baig YC, Paust S, Kim D, Kim S, Jia F *et al:* **AIMp1**
741 **Potentiates TH1 Polarization and Is Critical for Effective Antitumor and Antiviral Immunity.** *Front*
742 *Immunol* 2017, **8**:1801.

743 75. Kim MS, Kim S, Myung H: **Degradation of AIMp1/p43 induced by hepatitis C virus E2 leads to**
744 **upregulation of TGF-beta signaling and increase in surface expression of gp96.** *PLoS One* 2014,
745 **9**(5):e96302.

746 76. Bouhaddou M, Memon D, Meyer B, White KM, Rezelj VV, Correa Marrero M, Polacco BJ, Melnyk JE, Ulferts
747 S, Kaake RM *et al:* **The Global Phosphorylation Landscape of SARS-CoV-2 Infection.** *Cell* 2020,
748 **182**(3):685-712 e619.

749 77. Spalinger MR, Hai R, Li J, Santos AN, Nordgren TM, Tremblay ML, Eckmann L, Hanson E, Scharl M, Wu X
750 *et al:* **Identification of a Novel Susceptibility Marker for SARS-CoV-2 Infection in Human Subjects and**
751 **Risk Mitigation with a Clinically Approved JAK Inhibitor in Human/Mouse Cells.** *bioRxiv* 2020.

752 78. Taschuk F, Cherry S: **DEAD-Box Helicases: Sensors, Regulators, and Effectors for Antiviral Defense.**
753 *Viruses* 2020, **12**(2).

754 79. Wang P, Zhu S, Yang L, Cui S, Pan W, Jackson R, Zheng Y, Rongvaux A, Sun Q, Yang G *et al:* **Nlrp6**
755 **regulates intestinal antiviral innate immunity.** *Science* 2015, **350**(6262):826-830.

756 80. Mosallanejad K, Sekine Y, Ishikura-Kinoshita S, Kumagai K, Nagano T, Matsuzawa A, Takeda K, Naguro I,
757 Ichijo H: **The DEAH-box RNA helicase DHX15 activates NF-kappaB and MAPK signaling downstream**
758 **of MAVS during antiviral responses.** *Sci Signal* 2014, **7**(323):ra40.

759 81. Patabhi S, Knoll ML, Gale M, Jr., Loo YM: **DHX15 Is a Coreceptor for RLR Signaling That Promotes**
760 **Antiviral Defense Against RNA Virus Infection.** *J Interferon Cytokine Res* 2019, **39**(6):331-346.

761 82. Wang Y, Wu X, Ge R, Song L, Li K, Tian S, Cai L, Liu M, Shi W, Yu G *et al:* **Global Screening of Sentrin-**
762 **Specific Protease Family Substrates in SUMOylation.** *bioRxiv* 2020:2020.2025.964072.

763 83. Lord CJ, Ashworth A: **PARP inhibitors: Synthetic lethality in the clinic.** *Science* 2017, **355**(6330):1152-
764 1158.

765 84. Yelamos J, Monreal Y, Saenz L, Aguado E, Schreiber V, Mota R, Fuente T, Minguela A, Parrilla P, de
766 **Murcia G *et al:* PARP-2 deficiency affects the survival of CD4+CD8+ double-positive thymocytes.**
767 *EMBO J* 2006, **25**(18):4350-4360.

768 85. Obaji E, Haikarainen T, Lehtio L: **Characterization of the DNA dependent activation of human**
769 **ARTD2/PARP2.** *Sci Rep* 2016, **6**:34487.

770 86. Benchoua A, Couriaud C, Guegan C, Tartier L, Couvert P, Friocourt G, Chelly J, Menissier-de Murcia J,
771 **Onteniente B: Active caspase-8 translocates into the nucleus of apoptotic cells to inactivate**
772 **poly(ADP-ribose) polymerase-2.** *J Biol Chem* 2002, **277**(37):34217-34222.

773 87. Li S, Zhang Y, Guan Z, Li H, Ye M, Chen X, Shen J, Zhou Y, Shi ZL, Zhou P *et al:* **SARS-CoV-2 triggers**
774 **inflammatory responses and cell death through caspase-8 activation.** *Signal Transduct Target Ther*
775 **2020, 5**(1):235.

776 88. Lin CW, Lin KH, Hsieh TH, Shiu SY, Li JY: **Severe acute respiratory syndrome coronavirus 3C-like**
777 **protease-induced apoptosis.** *FEMS Immunol Med Microbiol* 2006, **46**(3):375-380.

778 89. Xia T, Yi XM, Wu X, Shang J, Shu HB: **PTPN1/2-mediated dephosphorylation of MITA/STING promotes**
779 **its 20S proteasomal degradation and attenuates innate antiviral response.** *Proc Natl Acad Sci U S A*
780 2019, **116**(40):20063-20069.

781 90. Nishiyama-Fujita Y, Shimizu T, Sagawa M, Uchida H, Kizaki M: **The role of TC-PTP (PTPN2) in**
782 **modulating sensitivity to imatinib and interferon-alpha in CML cell line, KT-1 cells.** *Leuk Res* 2013,
783 **37**(9):1150-1155.

784 91. Heinonen KM, Nestel FP, Newell EW, Charette G, Seemayer TA, Tremblay ML, Lapp WS: **T-cell protein**
785 **tyrosine phosphatase deletion results in progressive systemic inflammatory disease.** *Blood* 2004,
786 **103**(9):3457-3464.

787 92. Prescott L: **SARS-CoV-2 3CLpro whole human proteome cleavage prediction and**
788 **enrichment/depletion analysis.** *bioRxiv* 2020:2020.2008.2024.265645.

789 93. Bienert S, Waterhouse A, de Beer TA, Tauriello G, Studer G, Bordoli L, Schwede T: **The SWISS-MODEL**
790 **Repository-new features and functionality.** *Nucleic Acids Res* 2017, **45**(D1):D313-D319.

791 94. Wickham H, Averick M, Bryan J, Chang W, McGowan LD, François R, Grolemund G, Hayes A, Henry L,
792 Hester J *et al*: **Welcome to the Tidyverse.** *Journal of Open Source Software* 2019, **4**(43):1686.

793 95. ggrepel: Automatically Position Non-Overlapping Text Labels with 'ggplot2'. R package version 0.8.2.
794 [https://CRAN.R-project.org/package=ggrepel]

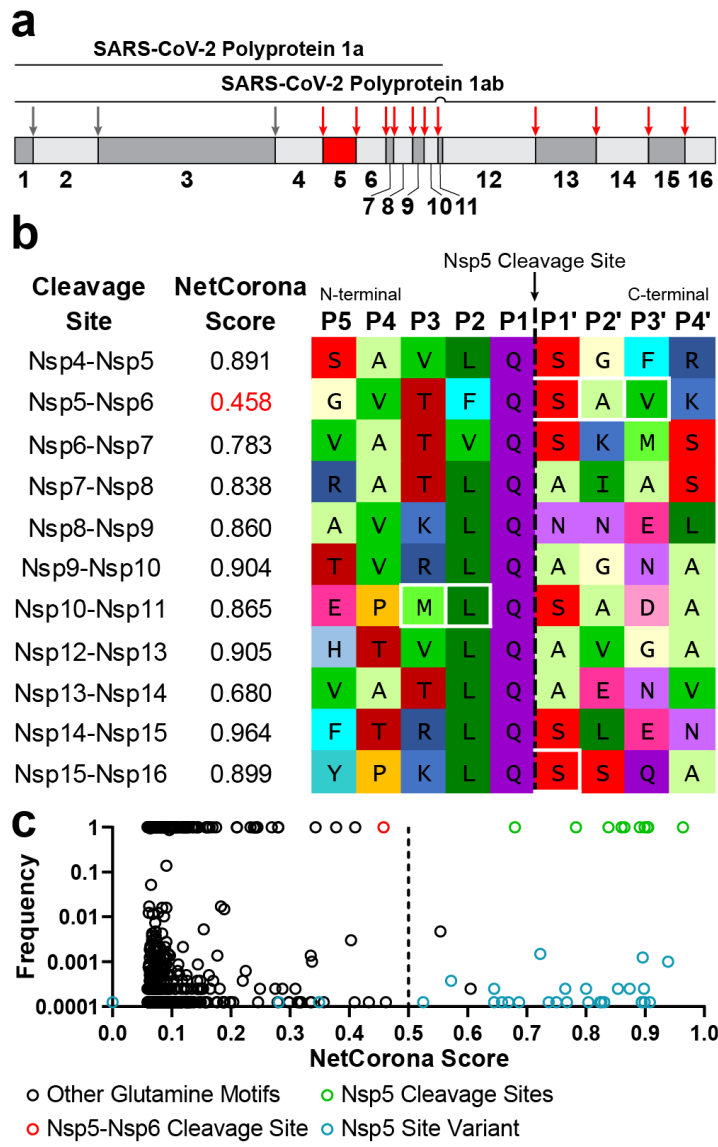
795 96. Uhlen M, Fagerberg L, Hallstrom BM, Lindskog C, Oksvold P, Mardinoglu A, Sivertsson A, Kampf C,
796 Sjostedt E, Asplund A *et al*: **Proteomics. Tissue-based map of the human proteome.** *Science* 2015,
797 **347**(6220):1260419.

798

799

800

801 **Figures**

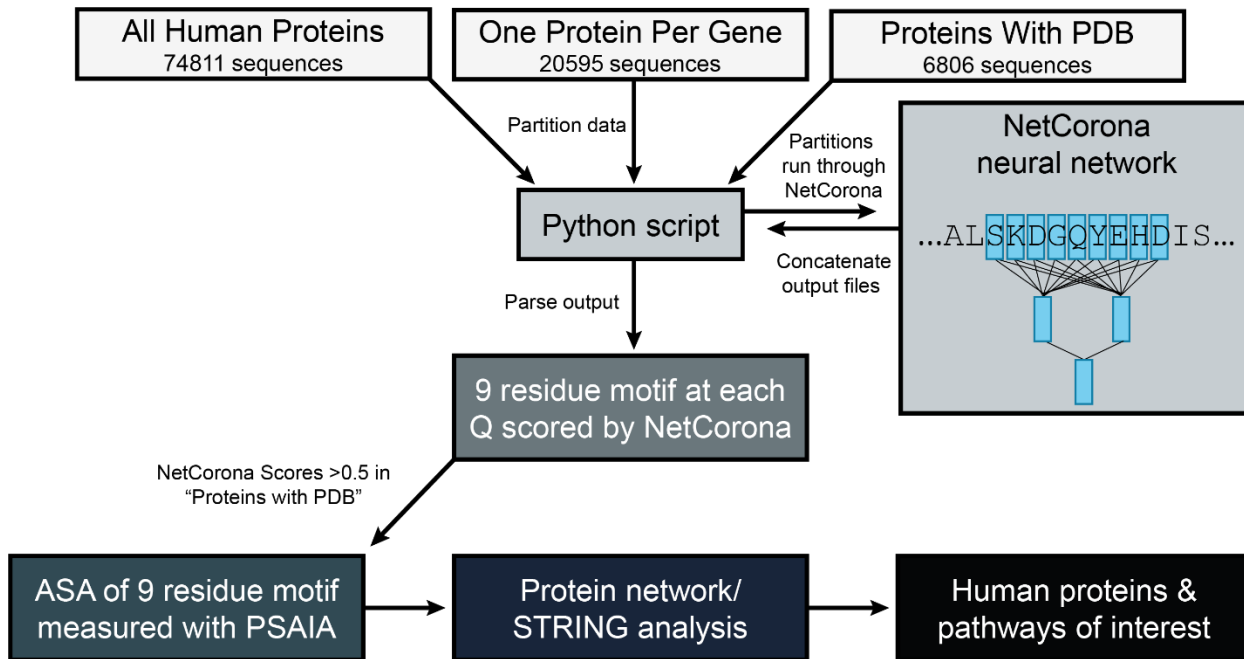


802

803

804 **Fig. 1 (a) The SARS-CoV-2 1a and 1ab polyproteins.** 1a contains Nsp1-Nsp11, 1ab contains
805 Nsp1-Nsp16 with Nsp11 skipped by a -1 ribosomal frameshift. Nsp5 and its cleavage sites are
806 indicated with red arrows. Nsp3 cleavage sites are indicated with grey arrows. **(b) SARS-CoV-2**
807 **native Nsp5 cleavage motifs.** NetCorona scores are indicated, and residues in white boxes
808 differ from SARS-CoV. **(c) SARS-CoV-2 1ab sequences scored with NetCorona.** Scores and
809 frequency were determined for all P5-P4' motifs surrounding glutamine residues in 8017 patient-
810 derived SARS-CoV-2 sequences. Known Nsp5 cleavage sites are indicated in green, while
811 mutations at a Nsp5 cleavage site are indicated in blue. The Nsp5-Nsp6 cleavage site is
812 indicated in red, and all other glutamine motifs are indicated in black.

813



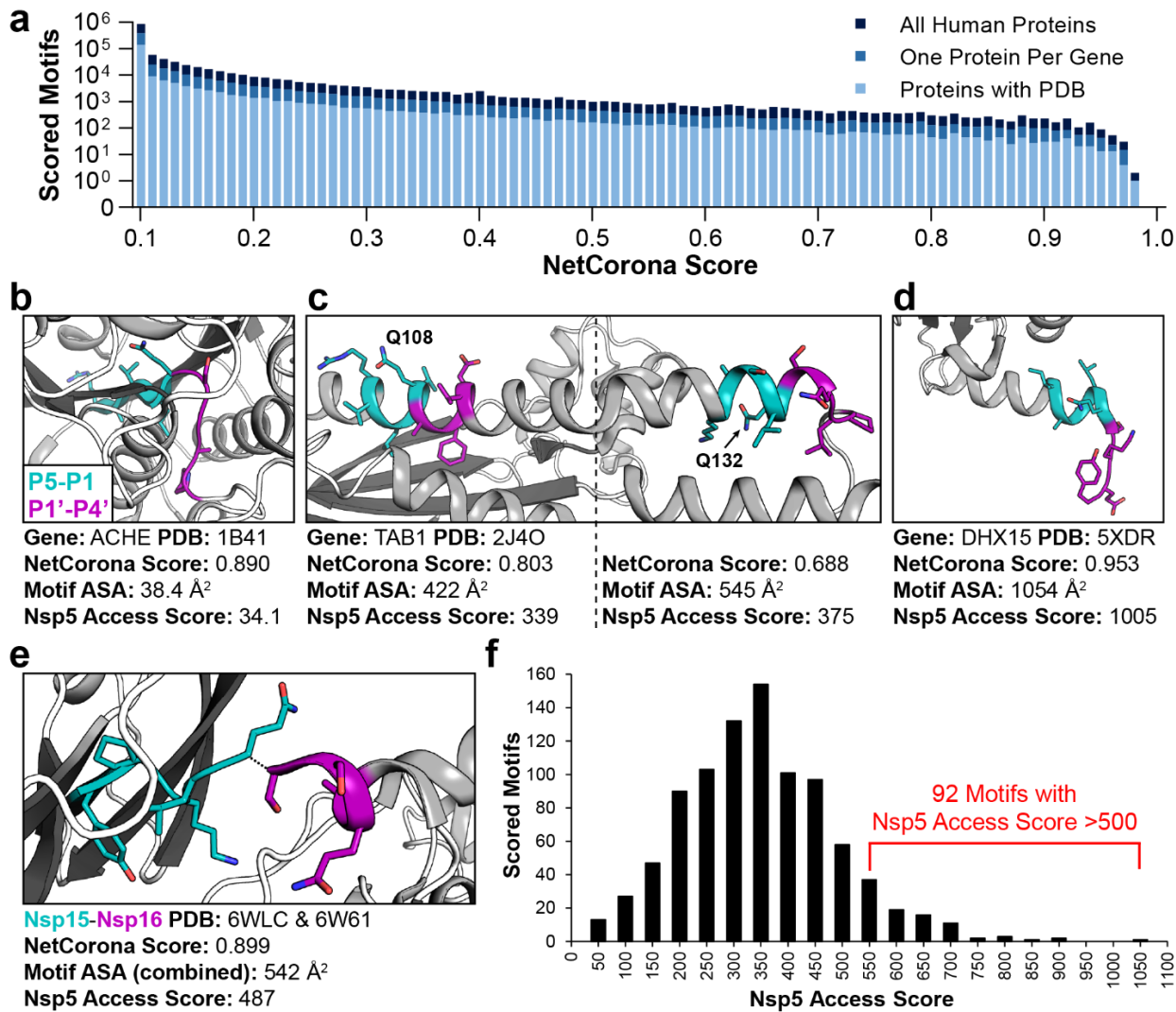
814

815

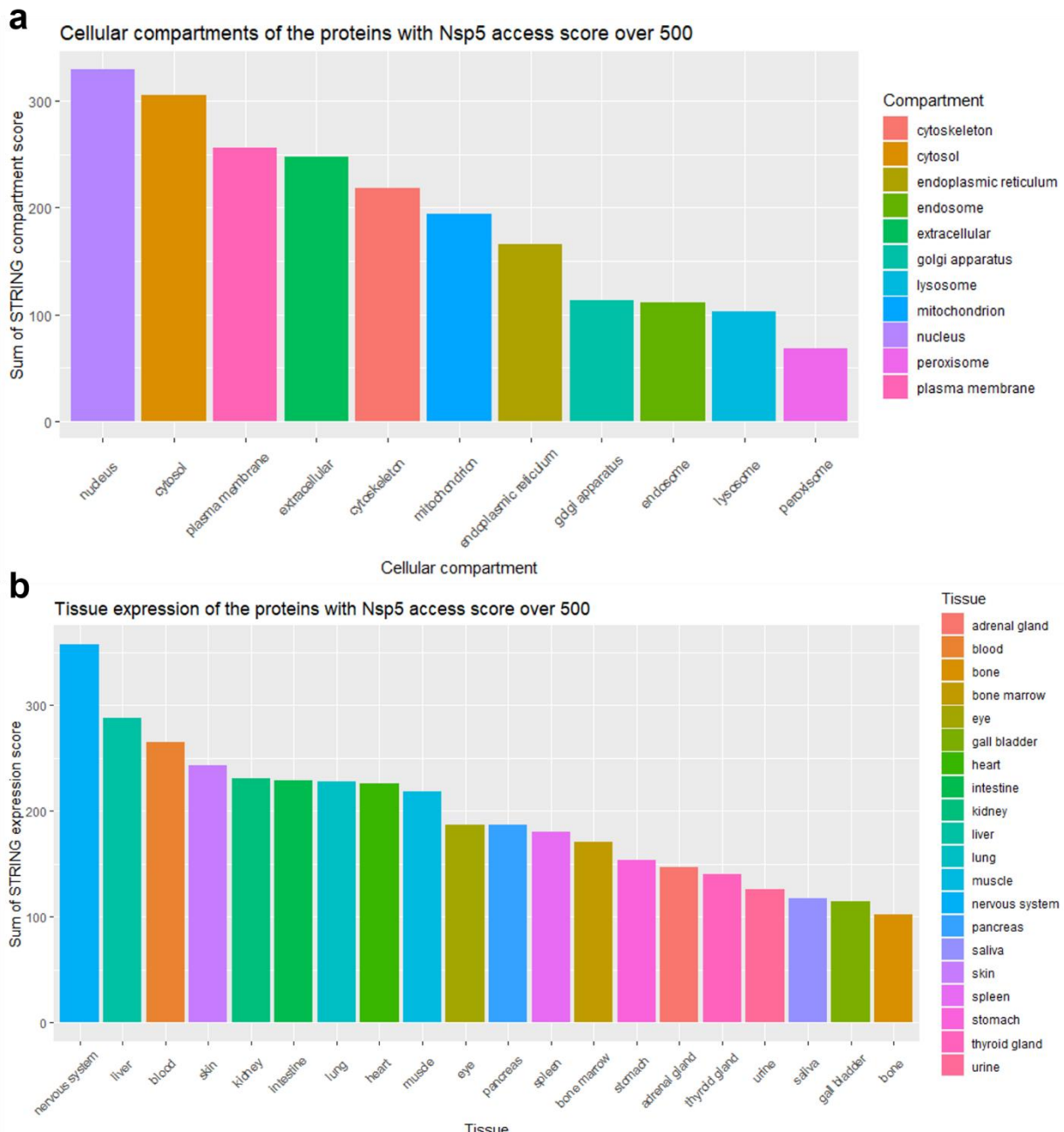
816 **Fig. 2 Overview of approach to predicting Nsp5 cleavage sites in human proteins.** Three
817 datasets of human protein sequences were analyzed by the NetCorona neural network.
818 NetCorona assigned scores (0 – 1.0) to the 9 amino acid motif surrounding every glutamine
819 residue in the datasets, where a score >0.5 was inferred to be a possible cleavage site. PDB
820 files associated with predicted cleaved proteins were analyzed using the Protein Structure and
821 Interaction Analyzer (PSAIA) tool, which output the accessible surface area (ASA) of each
822 predicted 9 amino acid cleavage motif. Proteins with highly predicted Nsp5 cleavage sites were
823 then analyzed using STRING, which provided information on tissue expression, subcellular
824 localization, and performed protein network analysis. Human proteins and molecular pathways
825 of interest containing a predicted Nsp5 cleavage site were then flagged for potential
826 physiological relevance.

827

828



829 **Fig. 3 Structural analysis of predicted and known Nsp5 cleavage motifs. (a)** NetCorona
 830 scores are shown for all P5-P4' motifs surrounding glutamine residues in three datasets of
 831 human proteins, binned by score differences of 0.01. The distributions of scores were not
 832 statistically different from one another. **(b)** Despite a high NetCorona score in ACHE, the motif's
 833 location in the core of the protein leads to a low Nsp5 access score. **(c)** TAB1 contains several
 834 motifs predicted to be cleaved, including at Q108 and Q132. The Nsp5 access score is slightly
 835 higher for the Q132 motif due to the greater accessible surface area (ASA). **(d)** DHX15 contains
 836 the motif with the highest Nsp5 access score observed in the human proteins studied, located
 837 on the C-terminus of the protein. **(e)** SARS-CoV-2 proteins Nsp15 and Nsp16 contain the native
 838 Nsp5 cleavage motif with the lowest Nsp5 access score calculated (487), which helped provide
 839 a cut-off to Nsp5 access scores in human proteins. **(f)** The Nsp5 access score of human protein
 840 motifs are indicated, binned by score differences of 50. 92 motifs in 92 unique human proteins
 841 have a Nsp5 access score >500.

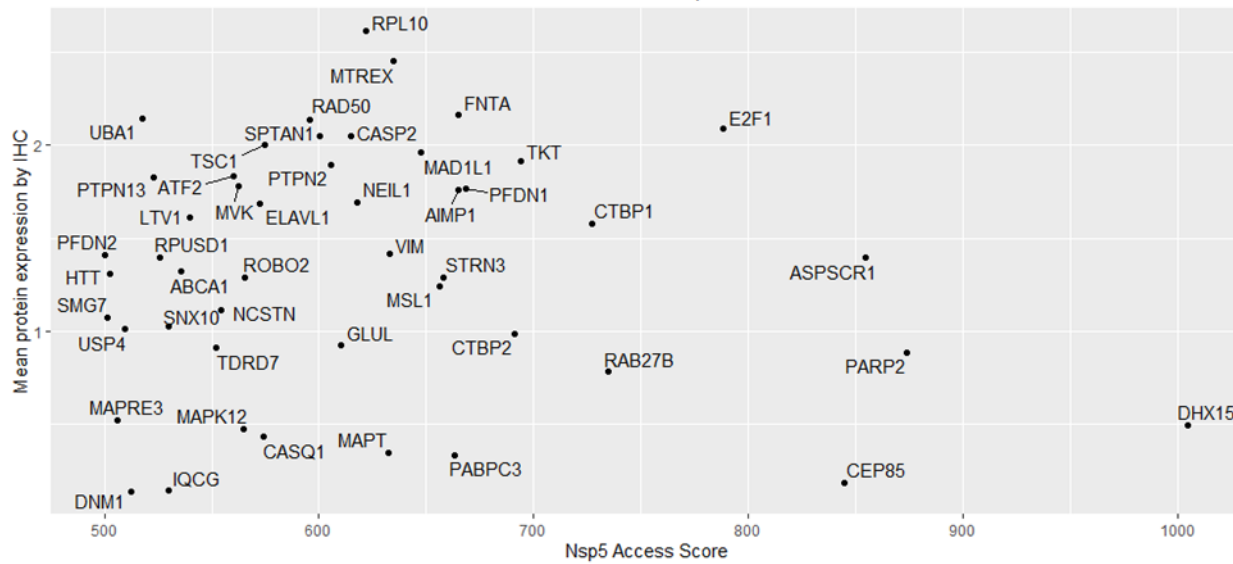


843

844 **Fig. 4** Sum of the compartment score (a) or expression score (b) of all human proteins with a
845 Nsp5 access score above 500 (92 proteins). Both the compartment and the expression score
846 were obtained from STRING based on text-mining and database searches.

847

Relationship between the Nsp5 Access Score and the average protein expression by IHC for protein with an Access Score of 500 or more, that are found in known Nsp5 subcellular locations



848

849 **Fig. 5** Proteins with a Nsp5 access score of 500 or more, that could be found in the same
850 cellular compartment as Nsp5 (48 proteins), were plotted against their expression in the human
851 body. For each protein, the mean expression by IHC is the mean across all tissues measured
852 and reported in the HPA (Not detected = 0, Low = 1, Medium = 2, High = 3, Not measured = NA
853 [which were ignored/removed]).

854

855

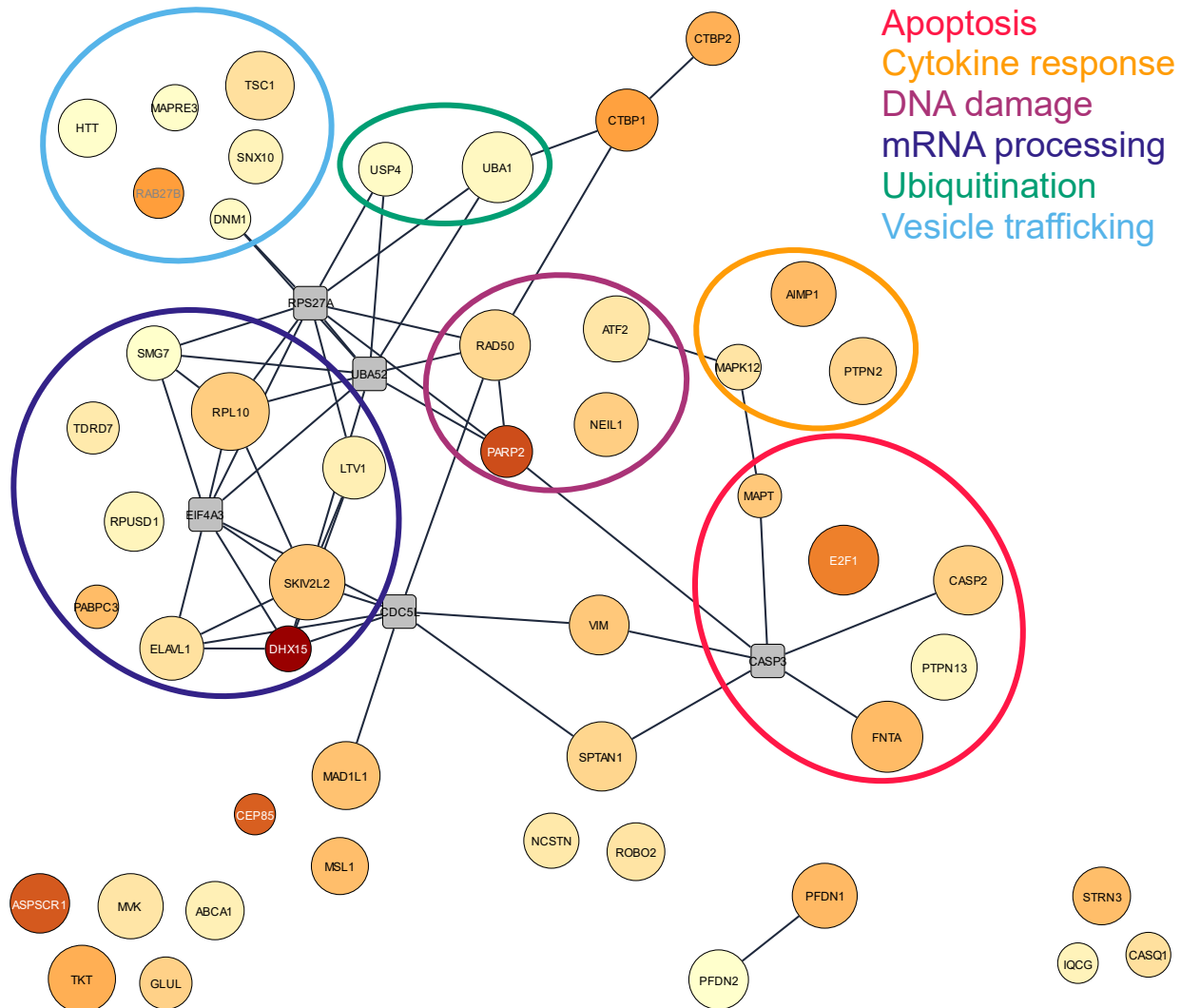
856

857

858

859

860



861 **Fig. 6 Network of proteins with plausible Nsp5 colocalization a Nsp5 access score above**
862 **500.** Node color represents the Nsp5 access score (light yellow = 500, dark red = 1005). Node
863 size indicates the mean expression across all tissue. Edge linking two nodes notes a known
864 interaction between these proteins. Grey squares are proteins added by STRING to add
865 connectivity to the network, but do not have an access score above 500 and/or plausible
866 colocalization with Nsp5. Circles highlighting pathways were based on STRING gene set
867 enrichment analysis coupled with manual searches in databases (Uniprot, GeneCARD,
868 PubMed).

869
870
871
872

873 **Additional Files**

874 Additional files are available here: <https://doi.org/10.6084/m9.figshare.14751306>

875

876 **Additional File 1:** This includes Supplementary Tables S1-S15

877

878 **Additional File 2:** human_all_proteins_netcorona.txt (108MB)

879 This is the raw data output by NetCorona following analysis of the “All Human Proteins” dataset

880

881 **Additional File 3:** human_one_gene_netcorona.txt (46MB)

882 This is the raw data output by NetCorona following analysis of the “One Protein Per Gene”
883 dataset

884

885 **Additional File 4:** dataset human_w_PDB_netcorona.txt (16MB)

886 This is the raw data output by NetCorona following analysis of the “Proteins With PDB” dataset

887

888 **Additional File 5: Figure S1** interaction scores vs max NetCorona score.pdf

889 Nsp5-human protein interaction data from Samavarchi-Tehrani *et al.* [51], plotted against the
890 maximum NetCorona score for human proteins from the “One Protein Per Gene” dataset.

891

892 **Additional File 6:** matching predicted motif to PDB.xlsx

893 Raw data displaying how predicted cleaved motifs were matched to a PDB file

894

895 **Additional File 7: Figure S2** ASA vs NetCorona score.pdf

896 Accessible surface area (ASA) of a predicted and known Nsp5 motifs plotted against NetCorona
897 scores, with data published by Moustaqil *et al.* and Koudelka *et al.* highlighted [46, 47], and the
898 Nsp5 access score cut-off displayed.